Molecular Catalysis 492 (2020) 111037

Contents lists available at ScienceDirect

Molecular Catalysis

journal homepage: www.elsevier.com/locate/mcat

Design and development of natural and biocompatible raffinose-Cu_2O magnetic nanoparticles as a heterogeneous nanocatalyst for the selective oxidation of alcohols

Mir Saeed Esmaeili (MS Student), Zahra Varzi (MS Student), Reza Eivazzadeh-Keihan (Phd Student), Ali Maleki (Professor)*, Hossein Ghafuri (Associate professor)*

Catalysts and Organic Synthesis Research Laboratory, Department of Chemistry, Iran University of Science and Technology, Tehran, 16846-13114, Iran

ARTICLE INFO

Keywords:
Magnetic nanocatalyst
Raffinose
Oligosaccharide
Oxidation reaction
Copper nanoparticles

ABSTRACT

Natural polymers are recently playing a vital role as a support for the noble metals. In the present study, raffinose from the classes of oligosaccharide polymer with a high capacity of magnetization was used as active support for the copper metal. The copper immobilized on the raffinose-based magnetic nanoparticles (MNPs) which can be used as a recyclable heterogeneous nanocatalyst for the selective oxidation of primary benzyl alcohols (PBA) to benzaldehyde (BAD) derivatives. The morphology and structure of the recoverable magnetic nanocatalyst were characterized using different microscopic and spectroscopic techniques including FT-IR, GC, VSM, XRD, TEM, TGA, FESEM and EDS analyses. Also, the optimum conditions of co-reactant, reaction time, oxidant, temperature and amount of the nanocatalyst for oxidation reaction were investigated. Moreover, the Fe_3O_4@raffinose-Cu_2O NPs had a significant effect to enhance yield and reduce the reaction time.

1. Introduction

The selective oxidation of alcohol mainly primary benzyl alcohols (PBA) to benzaldehyde (BAD) is one of the essential functional group transformations. BAD is a simplest aromatic aldehyde that exists in nature and a valuable raw material to start the preparation of perfumery, pharmaceutical and extensively used as the precursor for many fragrances, drugs, vitamins, dyes and pesticides [1,2]. Formerly, this conversion is carried out with permanganate and dichromate, but these reagents are poisonous that cause producing large amounts of harmful by-products leading to significant environmental problems [3,4].

Natural compounds, chiefly oligosaccharide as an essential class of biological polymers are more noticeable due to their readily availability, inexpensiveness and biodegradability. Oligosaccharides are carbohydrates with the smallest chain with two monomers and the largest chain with twenty monomers which are joined by a diversity of O-glycosidic bonds [5–7]. There are various functional groups in the construction of oligosaccharides that cause being capable of interacting with metal ions and nanoparticles (NPs). Due to the exclusive properties of oligosaccharide, they are appropriate candidates for the supporting applications in the heterogeneous catalytic systems [8].

Raffinose is a natural oligosaccharide constituted of galactose, fructose, and glucose sugar units (Fig. 1). The structure of raffinose is composed of galactose linked to the glycosylic group of sucrose via α-1,6 linkages. Raffinose is one of the available commercial trisaccharides that is the target of the new investigations; because it is the second natural abundant oligosaccharide after the sucrose in the agricultural and plant products [9]. Also, the main sources of raffinose are honey, leaves of the yew, potatoes, grapes, the seeds of numerous leguminous plants, and chiefly extracted from molasses. Furthermore, raffinose has been utilized as a pharmaceutically acceptable carrier a cryoprotectant for biopharmaceutics, and a prevailing elemental of maintenance solution for biological materials or organs in clinical transplantation [10,11].

In the recent decade, a rapid growth in the development of nanoscience were developed in various fields of chemistry such as nanomedicine and nanocarrier applications [12,13], nanobiosensor [14], nanowire [15] etc. Also nanoscience has played important roles in the synthesis and application of nanocatalysts as a progressive and expanding area [16]. Among the nanocatalysts, MNPs have found to be

* Corresponding author.
E-mail addresses: Mir_esmaeili@chem.iust.ac.ir (M.S. Esmaeili), zahra_varzi@chem.iust.ac.ir (Z. Varzi), Reza_eivazzadeh@chem.iust.ac.ir (R. Eivazzadeh-Keihan), maleki@iust.ac.ir (A. Maleki), Ghafuri@iust.ac.ir (H. Ghafuri).

https://doi.org/10.1016/j.mcat.2020.111037
Received 30 January 2020; Received in revised form 14 May 2020; Accepted 20 May 2020
2468-8231/ © 2020 Elsevier B.V. All rights reserved.

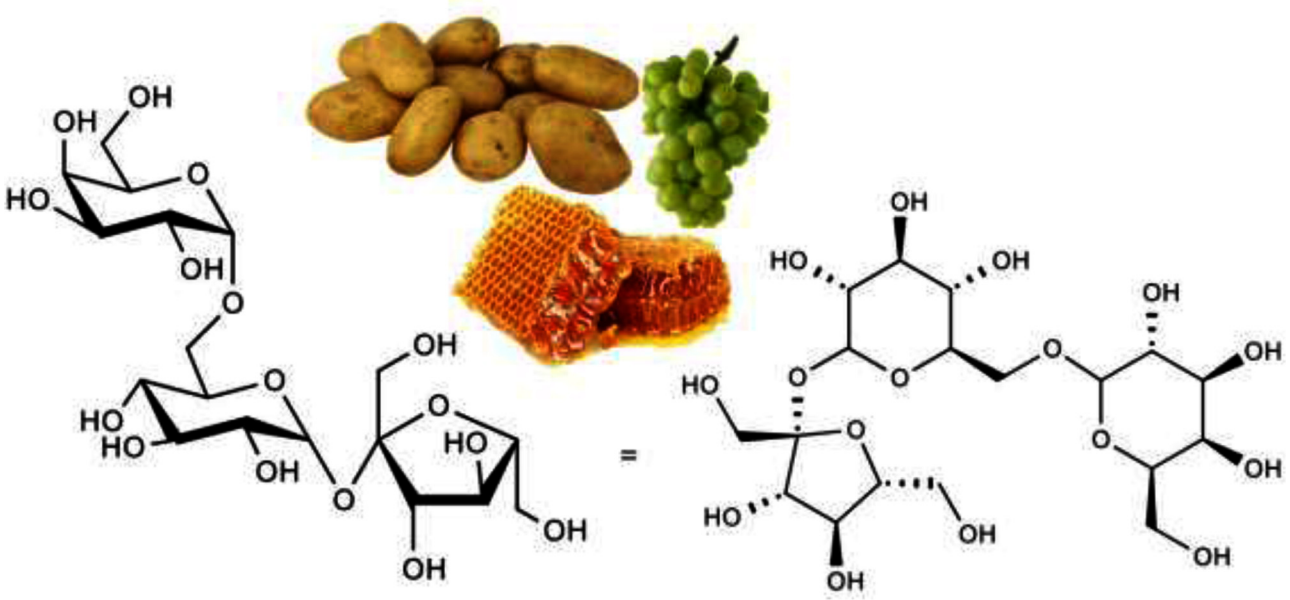

Fig. 1. Structure of raffinose.

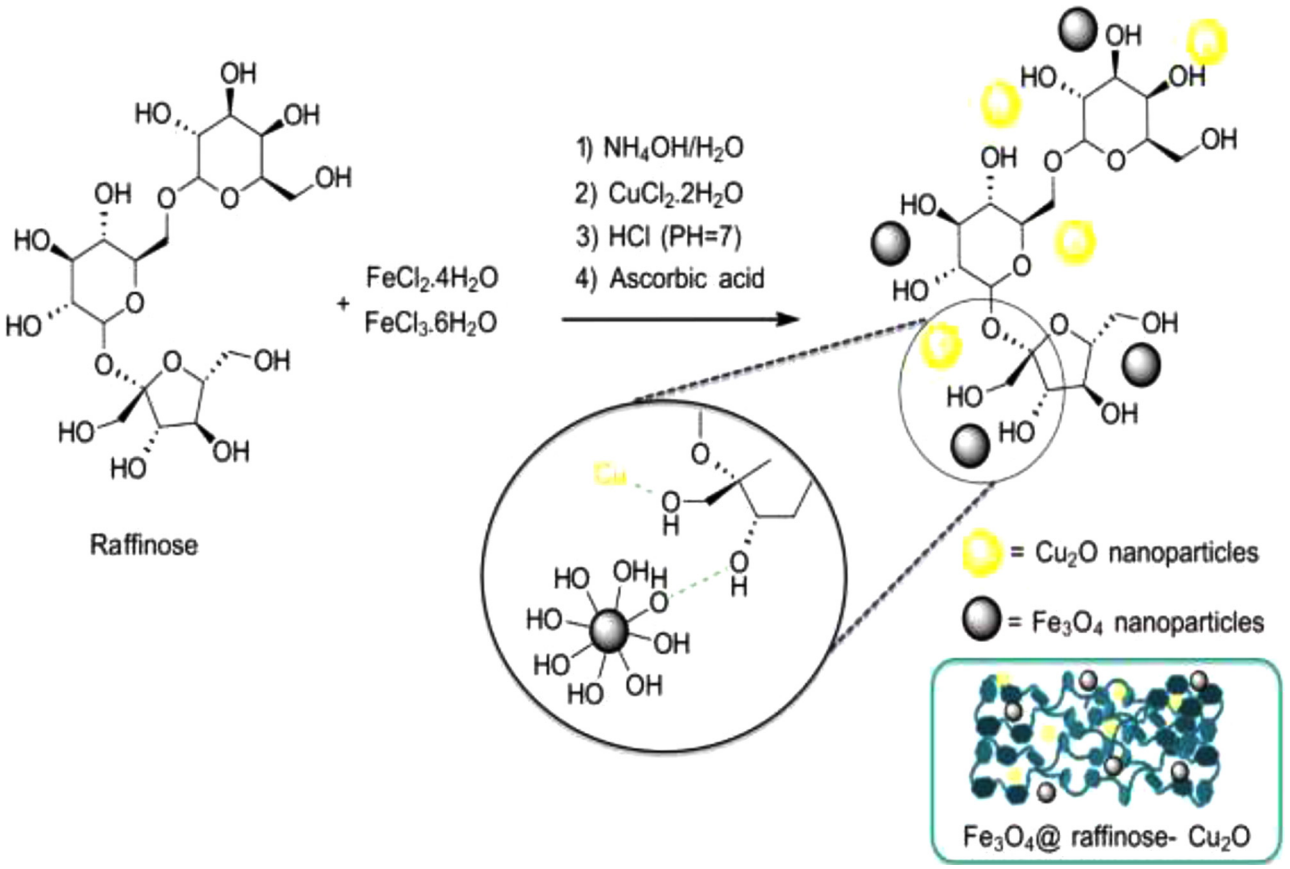

Fig. 2. Synthetic procedure of Fe_3O_4@raffinose-Cu_2O NPs.

more applicable in the organic reactions due to their easy separation [17,18], small size [19], excellent dispersion [20], low toxicity [21], reusability [22,23], cost-effective [24], high reactivity [25], remarkable chemical and physical stableness [26]. Therefore, MNPs play an important role as the catalyst support for the synthesis and catalysis in the field of green chemistry [27].

Several studies have been carried out on the compounds of noble metals as the catalytic systems. Moreover, a variety of transition metal catalysts such as Pd [2], Mn, Co, Ni, [4], Ag [28], Cu, Zn [29], etc. have been utilized for oxidation reactions of BA. Also, in comparison with other noble metals in the same probable applications, the copper NPs are valuable as a catalyst for the selective oxidation of PBA to BAD. This is because of their spread natural abundance, low price, high selectivity, nonpoisonous, excellent biocompatibility, and high catalytic performance [30–33]. In continuous our recent studies on MNPs, here in the raffinose-Cu_2O magnetic nanoparticles was reported as a

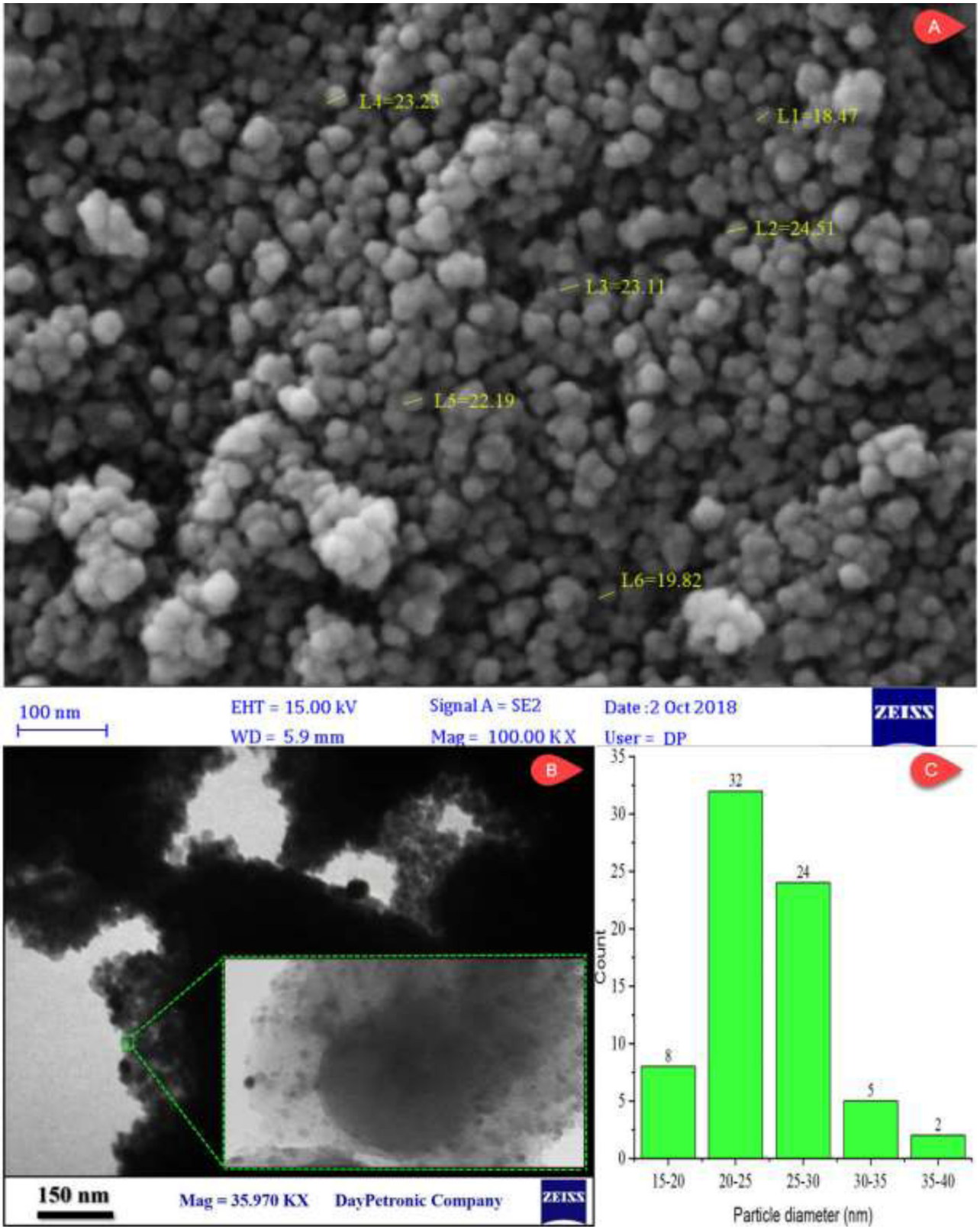

Fig. 3. (a) The FESEM image, (b) TEM image and (c) particle size distribution of the Fe_3O_4@raffinose-Cu_2O NPs.

recyclable, environmentally-benign and cost effective nanocatalyst. In the previous studies, the raffinose was not used for the catalytic applications but in the current study, the magnetized raffinose-based catalytic system is synthesized to oxidize PBA to BAD via immobilizing copper metal oxide. Also, various parameters were optimized to achieve high selectivity and conversion in this process.

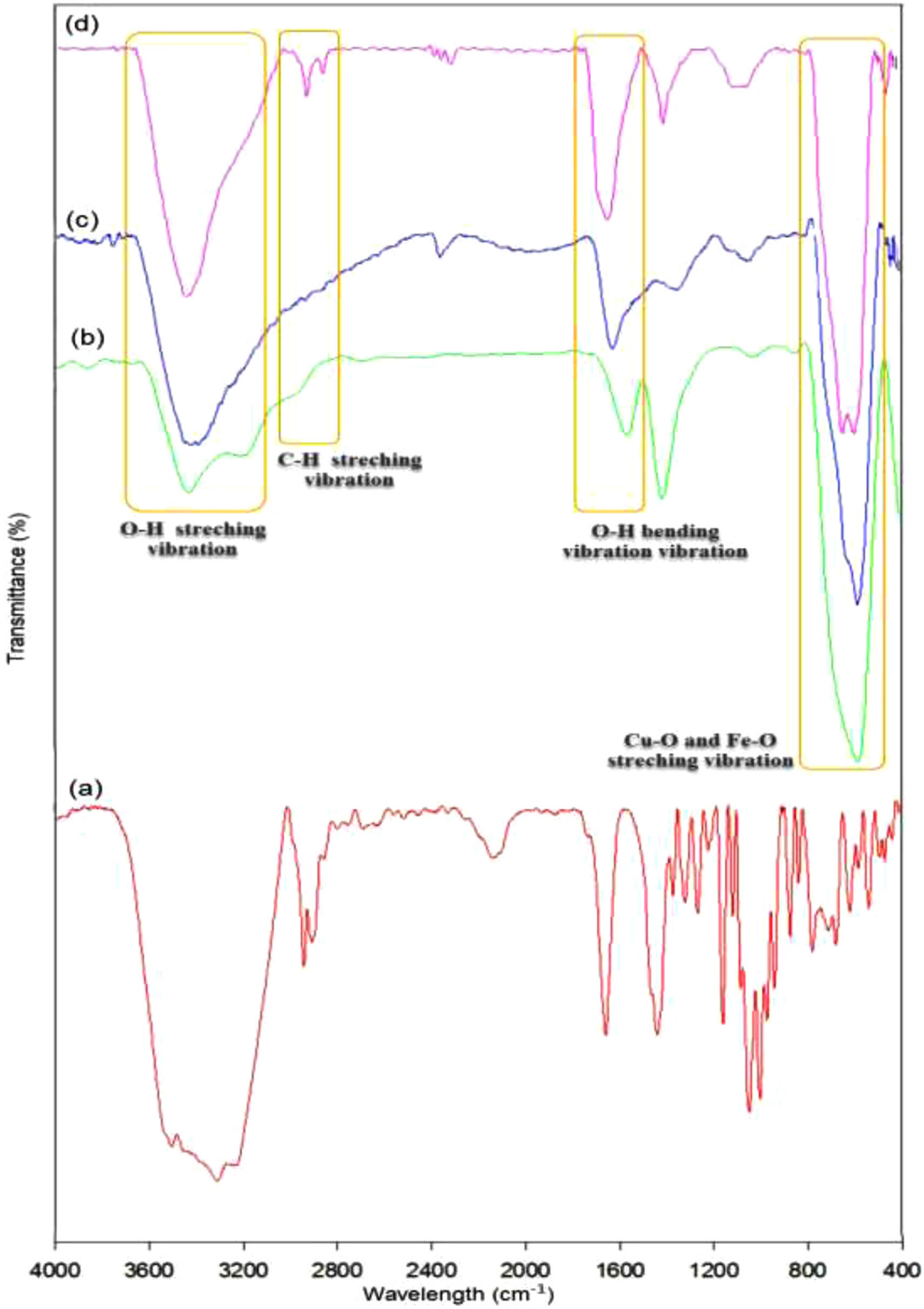

Fig. 4. The FT-IR spectra of (a) raffinose (b) Fe_3O_4 (c) Fe_3O_4@raffinose and (d Fe_3O_4@raffinose-Cu_2O NPs.

2. Materials and method

2.1. General remarks

Raffinose was purchased from Daejong and other chemical materials were supplied from Merck and used without further purification. The information of analysis devices is as follow: Energy-dispersive X-ray (EDX) analysis was recorded by TESCAN4992 device. FT-IR spectra of the biopolymer nanocatalyst were reported in the range of 400–4000 cm^{-1} using a Shimadzu IR-470 device. Gas chromatography (GC) recorded by a Shimadzu spectrometer. Powder X-ray diffraction (XRD) patterns of the biopolymer nanocatalyst were obtained using a PHILIPS-PW1730. Field emission scanning electron micrograph (FESEM) images of the biopolymer nanocatalyst were taken with a

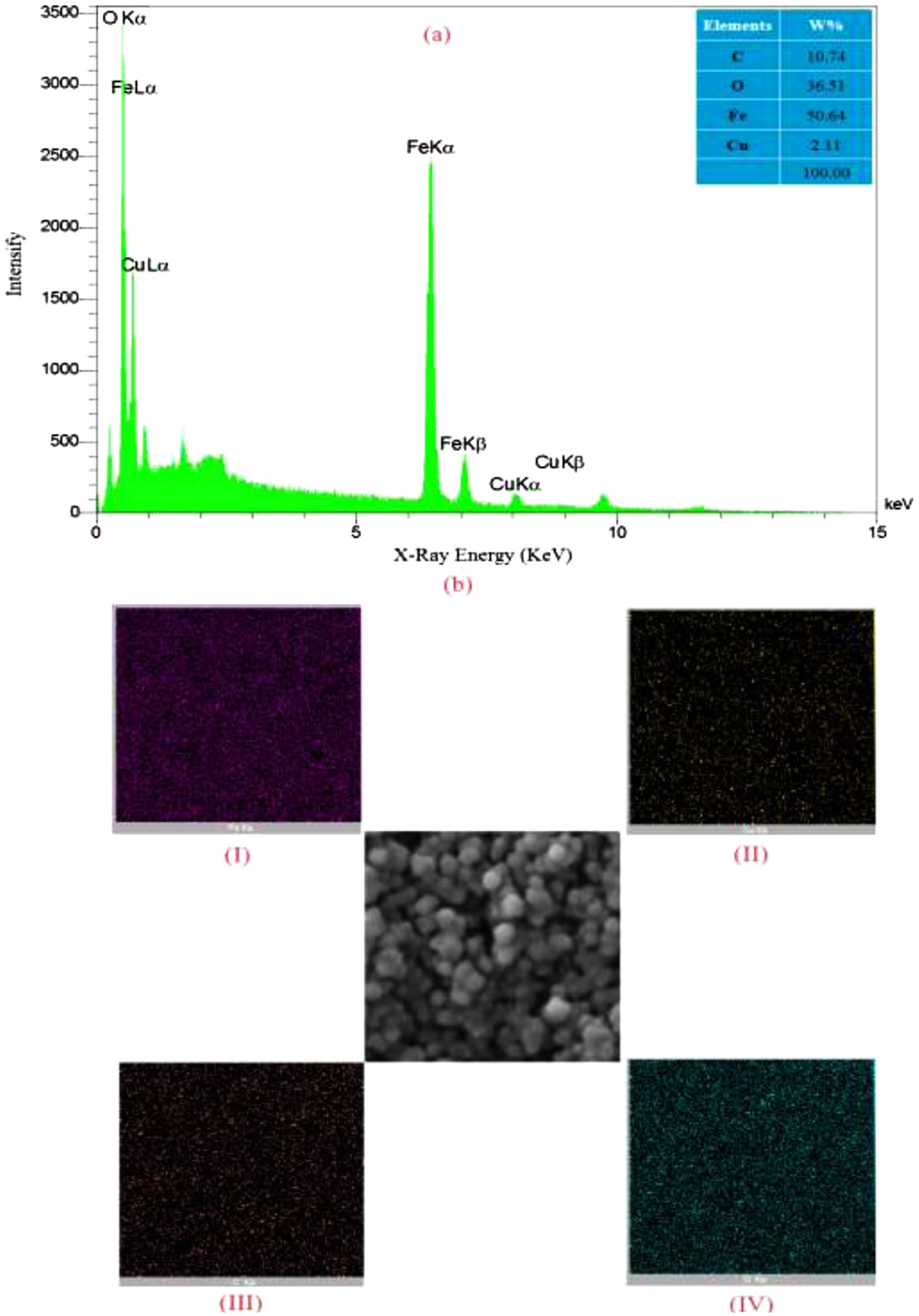

Fig. 5. (a) EDS spectra, and (b) elemental mapping images of (I) Fe, (II) Cu, (III) C and (IV) O of the Fe_3O_4@raffinose-Cu_2O NPs.

Sigma-Zeiss microscope. The transmission electron microscopy (TEM) image was achieved by Philips CM120. Magnetic measurements of the solid specimen were accomplished using an accurate magnetometer of Iran Kavir VSMs. Thermogravimetric analysis (TGA) was taken by the Bahr-STA504 instrument under the argon atmosphere.

2.2. Preparation of Fe_3O_4@raffinose-Cu_2O NPs

Raffinose with the amount of 0.8 g was mixed with 50 mL of water in a round bottom flask and the prepared mixture was stirred at 1000 rpm for 10 min to achieve a homogenous dispersion. Then, $FeCl_3{\cdot}6H_2O/FeCl_2{\cdot}4H_2O$ with the ratio of 2:1 (1.95 g/0.75 g) was slowly added into the mixture and temperature was slowly increased to

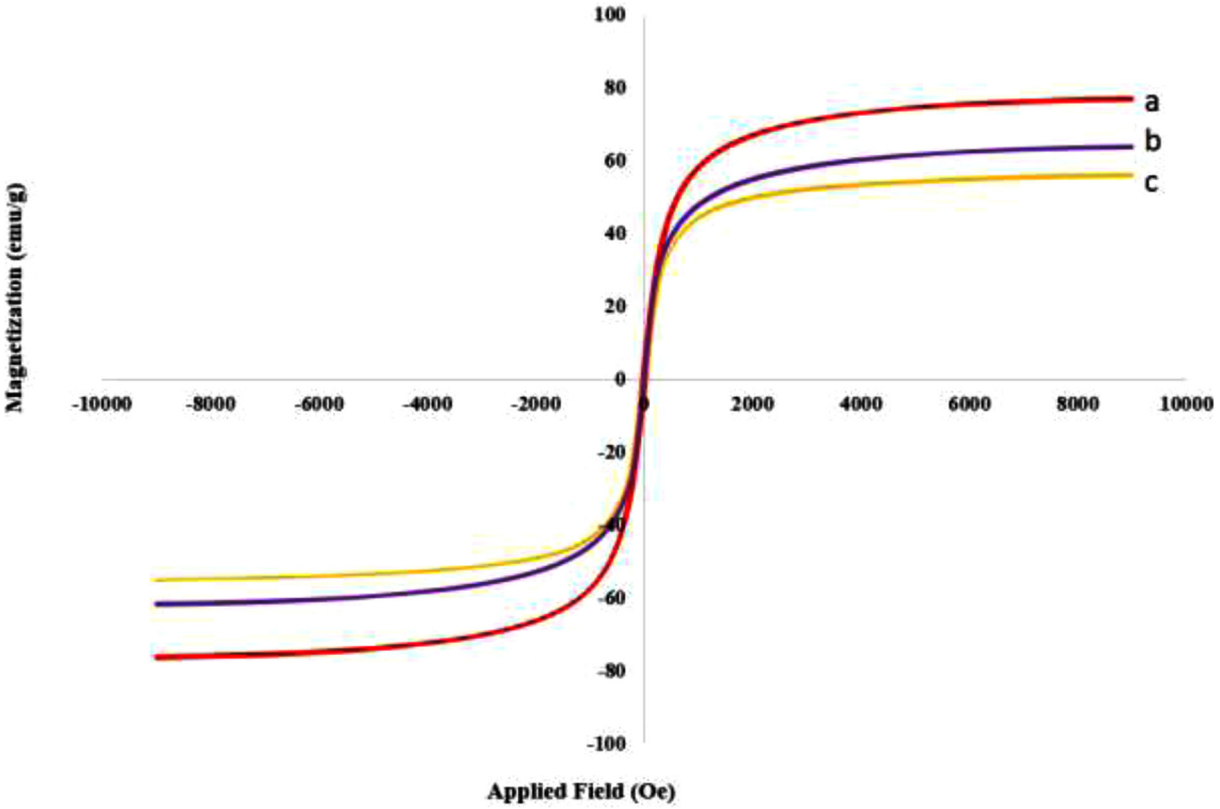

Fig. 6. VSM magnetization curves of the (a) Fe_3O_4, (b) Fe_3O_4@raffinose and (c Fe_3O_4@raffinose-Cu_2O NPs.

80 °C in a nitrogen atmosphere at a constant stirring of 1000 rpm for 30 min. In the next stage, aqueous ammonium hydroxide (25%) was instantaneously added to the homogeneous dispersed system until to reach pH = 12. The reaction mixture was then kept under the stirring for 1 h at 80 °C. In continuation, the solution was cooled and copper(II) chloride dehydrate (0.09 g, 0.5 mmol) was dissolved in 10 mL of deionized water and they were steadily added to the solution by stirring for 1 h at 80 °C. After that the reaction mixture was neutralized with 0.5 M hydrochloric acid solution, then ascorbic acid (50 mL, 0.05 M) was added slowly at the temperature of 80 °C and stirring condition for 36 h to yield Fe_3O_4@raffinose-Cu_2O NPs (Fig. 2). The obtained product was magnetized by a magnet and washed with ethanol three times and was dried at 60 °C for 6 h under vacuum conditions. Finally, the powder of Fe_3O_4@raffinose-Cu_2O NPs was prepared for the corresponding analyses.

2.3. General procedure for the selective oxidation of PBA to BAD using Fe_3O_4@raffinose-Cu_2O NPs

Fe_3O_4@raffinose-Cu_2O NPs (0.03 g), 4-methoxybenzyl alcohol (1 mmol) and tertbutyl hydroperoxide (TBHP) (1 mmol) with 0.5 mL acetonitrile were fed into a test tube equipped with a magnetic stirrer under refluxing conditions. After completion of the reaction, the biopolymer nanocatalyst was separated using a permanent magnet, washed, dried under the vacuum condition and accumulated for the next experiment without any other treatment.

3. Characterization of Fe_3O_4@raffinose-Cu_2O NPs

3.1. FESEM and TEM analysis

FESEM and TEM images of the catalyst are exhibit spherical morphologies and excellent dispersion of NPs in the polymeric matrix as shown in Fig. 3. MNPs can be seen as dark spots encapsulated by more bright raffinose and copper nanoparticles shells. Such spherical morphologies of the NPs have increased the surface area of nanocatalyst and enhanced the catalytic performance. Also, the size distribution of NPs was approximately in the range of 15 − 40 nm, with the average particle size of about 24 nm for 70 particles.

3.2. FT-IR spectroscopy

FT-IR spectra of raffinose, Fe_3O_4, Fe_3O_4@raffinose, and Fe_3O_4@raffinose-Cu_2O NPs are shown in Fig. 4. In the FT-IR spectrum of Fe_3O_4@raffinose-Cu_2O NPs, a strong adsorption band at a range of 550–750 cm^{-1}can be visible and it is appointed to the overlapping stretching vibration of Cu-O and Fe-O bands [34]. The adsorption band range of 2850–2950 is related to the C–H stretching vibrations. Furthermore, the adsorption bands at 1660 cm^{-1} and the range of 3223 − 3600 cm^{-1} are related to OH− bending vibration and stretching vibrations bands [35].

3.3. EDS analysis

The results of the EDS analysis of Fe_3O_4@raffinose-Cu_2O NPs is also depicted in Fig. 5a. Based on this figure, the existence of C, O, Fe and Cu elements are clear and it is proved that the copper on the surface of Fe_3O_4@raffinose is immobilized well. To approve the copper dispersion on the surface of the Fe_3O_4@rafinose, elemental mapping images was taken with the EDS device and presented in Fig. 5b. The homogeneous dispersion of copper on the nanocatalyst surface is also specified in the maps. Form the results, it was concluded that the nanocatalyst is well synthesized.

3.4. Vibrating sample magnetometer (VSM)

Magnetization curves of the nanocatalyst before and after immobilization of raffinose and Cu_2O are represented in Fig. 6. Based on

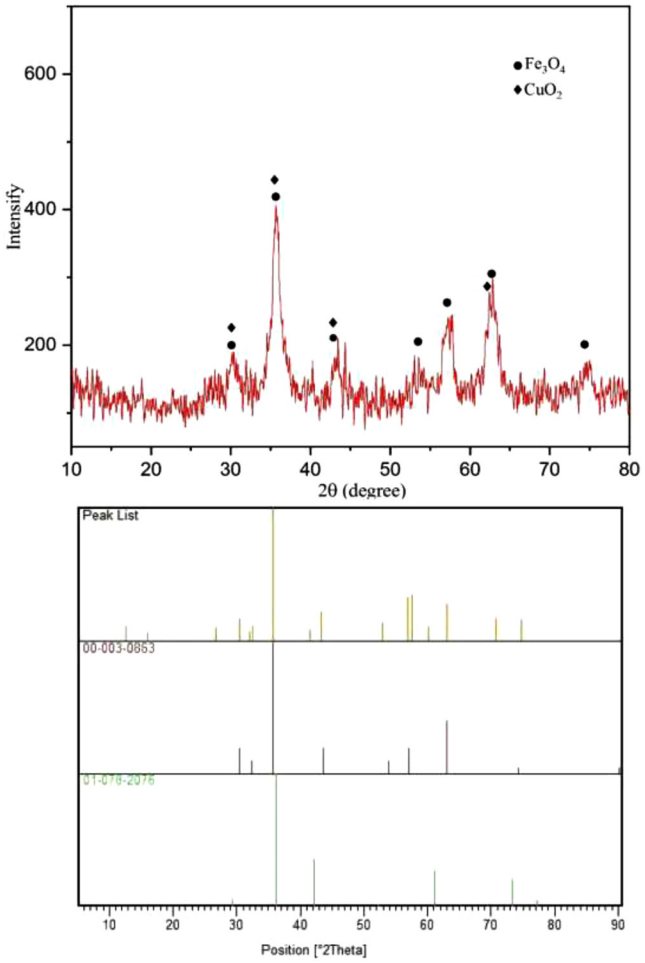

Fig. 7. The XRD pattern of the Fe_3O_4@raffinose-Cu_2O NPs.

the previous studies, the magnetic saturation value for Fe_3O_4 is 75 emu g^{-1} [36]. The reason for a reduction in magnetization value is typically attributed to the existence of newly loaded functional groups on the surface of the MNPs. As can be seen in Fig. 6 the magnetic saturation value of Fe_3O_4 is approximately 75 emu g^{-1} (Fig. 6a) that in comparison with a magnetic saturation value of Fe_3O_4@raffinose with 64 emu (Fig. 6b) and Fe_3O_4@raffinose-Cu_2O NPs (Fig. 6c) with 56 emu g^{-1} was decreased. Furthermore, the magnetic saturation value of Fe_3O_4@raffinose-Cu_2O NPs showed that novel nanocatalyst have a superparamagnetic action at room temperature and the VSM curve can confirm this effect.

3.5. X-ray diffraction (XRD)

The XRD pattern of Fe_3O_4@raffinose-Cu_2O is presented in Fig. 7. Six diffraction peaks at 2θ = 30.16°, 35.45°, 43.25°, 53.55°, 56.78°, and 62.73° were corresponded to (2 2 0), (3 1 1), (4 0 0), (4 2 2), (5 5 1) and (4 4 0) diffraction planes of magnetite (Fe_3O_4) NPs with cubic phase that was in excellent agreement with the reported JCPDS card no. 03-0863 [37]. Four distinguished diffraction peaks at 2θ = 29.58°, 36.42°, 42.34°, and 61.40° were related to (1 1 0), (1 1 1), (2 0 0) and (2 2 0) diffraction planes of Cu_2O that was in good acceptance with the reported JCPDS card no 78-2076 [38]. The XRD conclusion for the Fe_3O_4@raffinose-Cu_2O NPs expresses that the crystal arrangement of the Fe_3O_4 core does not convert throughout the functionalization route.

3.6. TGA

The TGA was performed to examine the thermal feature of the nanocatalyst. As indicated in Fig. 8, the TGA weight loss thermogram of the Fe_3O_4@raffinose-Cu_2O NPs exhibits three significant weight losses in the range of 50–800 °C which is equal to 15% weight of the nanocatalyst. The first small amount of weight loss around 100 °C was attributed to the desorption of adsorbed water. The second and third weight losses are related to the successful grafting of raffinose on the surface of the Fe_3O_4 NPs. These weight losses were showed in two parts in the range of 200 − 350 °C and 350 − 800 °C that the first range was relatively attributed to depolymerization and dehydration of oligosaccharide rings and the second was appointed to separation of the biopolymer matrix and cross-links among biopolymer chain.

3.7. Application of the Fe_3O_4@raffinose-Cu_2O NPs for the selective oxidation of PBA to BAD

A variety of substrates of electron-donating and electron-withdrawing groups were applied to study the performance and effectiveness of green Fe_3O_4@raffinose-Cu_2O NPs. The result of yield and reaction time for the selective oxidation of PBA to BAD is presented in Table 1. All the substrates were successfully converted to the corresponding BAD at high conversions of 87–97% without any byproducts such as aromatic acids within reaction times of 3–6.5 h.

3.8. Optimization of the selective oxidation of PBA to BAD

The refluxing conditions in the acetonitrile as a co-reactant was considered as a model reaction for the synthesis of the 4-methoxy benzaldehyde (**2f**) to evaluate the efficiency of Fe_3O_4@raffinose-Cu_2O NPs oxidation of 4-methoxybenzyl alcohol (**1f**) in the presence of TBHP. At first, the effects of various amounts of catalyst loading are investigated. Initial experiments depicted that the trace product of **2f** was converted in the absence of any catalyst even when the reaction substrate was stirred in the acetonitrile under reflux conditions for 3 h (Entry 1, Table 2). Interestingly, when a specified amount of a catalytic was added to the reaction mixture in the acetonitrile under refluxing conditions, the desired product of **2f** was obtained. According to the results of Table 2 entry 3, 4, 5 and 6, when 0.03 g amount of catalyst was added, the rate of the reaction and conversion values were higher for desired products at fewer reaction times. During the optimization examinations, different temperatures and co-reactant were investigated and it was found that the catalyst activity under refluxing conditions in the acetonitrile co-reactant is the best temperature and co-reactant amount between other tested conditions in terms of produced desired product of **2f** at a high conversion of 97% and lower reaction time of 3 h.

3.9. Proposed mechanism for the selective oxidation of PBA to BAD using Fe_3O_4@raffinose-Cu_2O NPs

The proposed mechanism for the selective oxidation of PBA to BAD in the presence of catalyst is shown in Fig. 9. In the first step, the copper NPs (**I**) has interacted with the acetonitrile (**II**) as a co-rectant to formed active nitrile intermediate (**III**). Then in the presence of TBHP (**IV**), intermediate **III** converted to the peroxyimidic acid (**V**) that is known as an active oxidant reagent and plays a considerable role during the oxidation reactions [39]. In the next step, most active part of the peroxyimidic acid reacts with PBA and formed intermediate **VII**. In order to form a sustainable product from intermediate **VII**, intramolecular exchange occurs to the formation of product **VIII**.

3.10. Reusability of Fe_3O_4@raffinose-Cu_2O NPs

The reusability of the nanocatalyst is an important issue based on

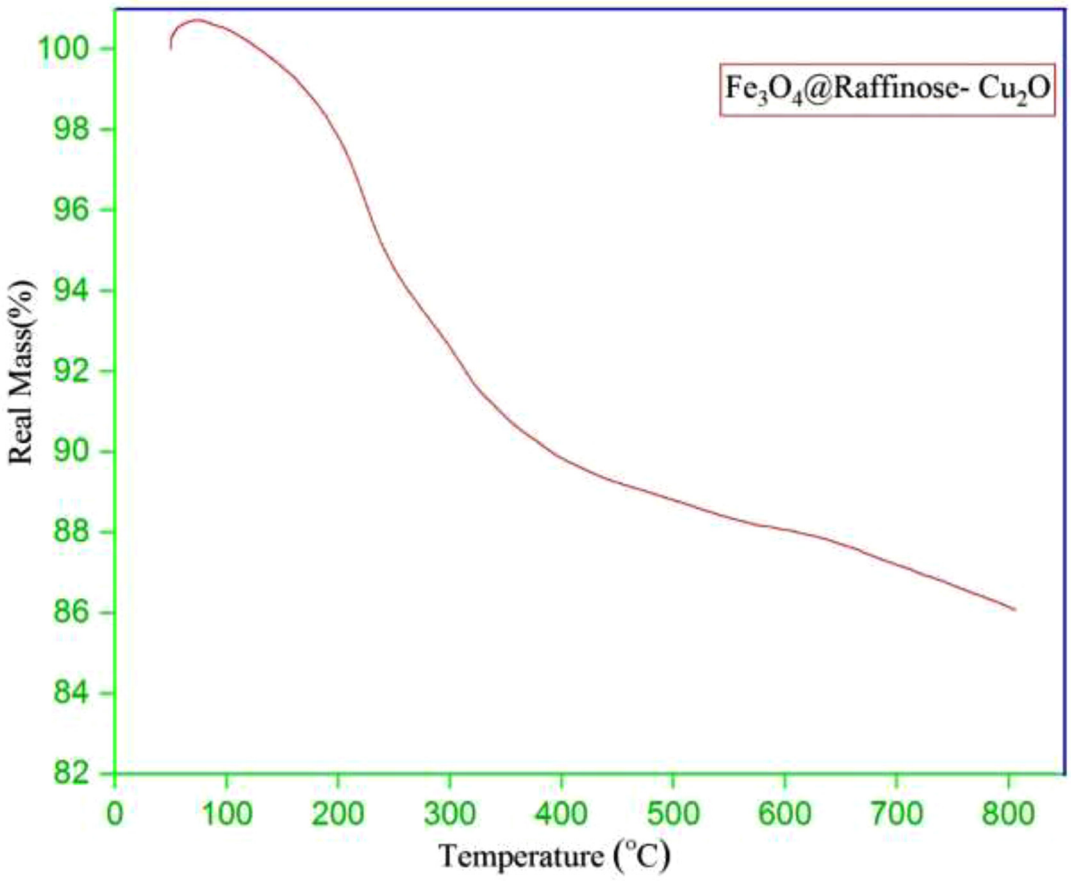

Fig. 8. The TGA of the Fe_3O_4@raffinose-Cu_2O NPs.

the laboratory and industrial applications viewpoint. Based on the obtained results, it was deduced that the nanocatalyst could be recovered and reused for six continuous cycles with an insignificant reduction in conversion from 97 to 84% as depicted in Fig. 10a. The FT-IR spectra, FESEM image and XRD analyses of the obtained catalyst after six times used in the model reaction were presented in Fig. 10b-c to study the structural variations of the nanocatalyst. A comparison between before and after six times used in the reaction shows that there is no difference between analyses. Also, no considerable loss of performance was observed for nanocatalyst after six cycles of reuse.

3.11. Comparison of catalyst

The efficiency of the Fe_3O_4@raffinose-Cu_2O NPs based on magnetic nanocatalyst was compared to previously reported catalysts in the literature. In Table 3, the selective oxidation of 4-methoxybenzyl alcohol to 4-methoxy benzaldehyde in the presence of the Fe_3O_4@raffinose-Cu_2O NPs was compared with other catalysts based on the reaction time (Table 3, Entries 1 and 2) and yield of the desired product (Table 3, Entries 1, 2, 3, 4 and 5). As can be seen, the present catalyst has less time and higher yield relative to the previous catalysts.

4. Conclusions

In summary, here in a novel, efficient, low-cost, and reusable Fe_3O_4@raffinose-Cu_2O NPs with a simple co-precipitate method was synthesized and applied as a nanocatalyst. In this work due to the presence of MNPs the nanocatalyst easily separated from the reaction without using conventional separation techniques such as filtration or centrifugation, then its combination with raffinose increased the thermal resistance of the synthetic nanocatalyst. Also, raffinose by having a large number of hydroxyl functional groups in its polymer chains, caused to immobilization of copper NPs on the surface of magnetic raffinose and stabilizes it during the chemical reaction. Copper as a fundamental component of the catalyst facilitated more the oxidation of PBA to BAD. Various techniques such as FT-IR, GC, VSM, TGA, XRD, TEM, FESEM, and EDS analyses were performed to characterize the synthesized heterogeneous nanocatalyst. The results of the FT-IR analysis technique were demonstrated the Fe-O and the Cu-O adsorption bands. The XRD pattern was exhibited diffraction peaks of Fe_3O_4 with the reported JCPDS card no. 03-0863 and Cu_2O with the reported JCPDS card no 78-2076 and approved that the heterogeneous nanocatalyst was successfully synthesized. Analysis of the EDS was confirmed the immobilization and dispersion of copper within the Fe_3O_4@raffinose structure. Furthermore, the monodispersed spherical particles with an average size of NPs among 24.5 nm were observed based on the FESEM and TEM images. The VSM analysis was depicted as a reduction in the amount of magnetization features of the Fe_3O_4 NPs by immobilization of the raffinose-Cu_2O on the Fe_3O_4. The obtained results from the TGA verified that the heterogeneous nanocatalyst in the organic reactions is suitable. The catalytic activity of Fe_3O_4@raffinose-Cu_2O NPs was evaluated in the selective oxidation of the PBA to BAD under refluxing conditions in acetonitrile. The fewer reaction time and higher yield were achieved for the present catalyst in comparison to the previous catalyst. The Fe_3O_4@raffinose-Cu_2O NPs were quickly separated and retained 84% of their activity after six cycles without remarkable loss of its performance and stability. As a main result, it is valuable to develop new catalytic systems based on the present raffinose as an important polysaccharide.

Table 1
Oxidation of PBA to BAD at the optimum conditions[a].

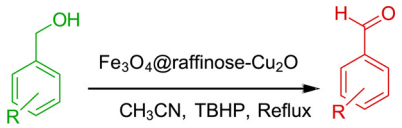

Entry	Reactant (PBA)	Product (BAD)	Time (h)	Conversion (%)[b]	Selectivity to BAD (%)
1	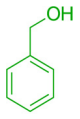 **1a**	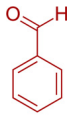 **2a**	4	94	> 99
2	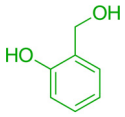 **1b**	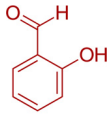 **2b**	4/30	95	> 99
3	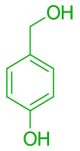 **1c**	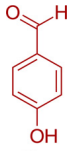 **2c**	3/5	96	> 99
4	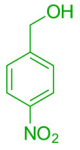 **1d**	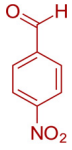 **2d**	6/5	87	> 99
5	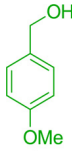 **1e**	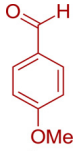 **2e**	3	97	> 99
6	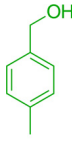 **1f**	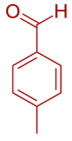 **2f**	4	95	> 99
7	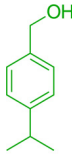 **1g**	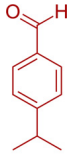 **2g**	4/5	94	> 99
8	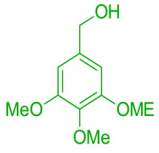 **1h**	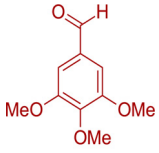 **2h**	3/5	96	> 99

[a] Reaction conditions: 4-methoxybenzyl alcohol (1.0 mmol), TBHP (1.0 mmol) and Fe_3O_4@raffinose-Cu_2O NPs (0.006 g) in 0.5 mL of acetonitrile under refluxing conditions.
[b] Selectivity and conversion determined by GC using biphenyl as an internal standard.

CRediT authorship contribution statement

Mir Saeed Esmaeili: Data curation, Investigation, Project administration, Resources, Software, Writing - original draft, Writing - review & editing. **Zahra Varzi:** Data curation, Formal analysis, Investigation, Methodology, Project administration, Resources, Writing - original draft, Writing - review & editing. **Reza Eivazzadeh-Keihan:** Investigation, Methodology. **Ali Maleki:** Funding acquisition, Project

Table 2
Optimization of the oxidation of PBA to BAD in the model reactions[a].

Entry	Amount of catalyst (g)	Oxidant (mmol)	Co-reactant	Temperature (°C)	Time (h)	Conversion (%)[b]
1	–	1	ACN	Reflux	3	Trace
2	0.03	1	–	Reflux	3	Trace
3	0.01	1	ACN	Reflux	3	58
4	0.02	1	ACN	Reflux	3	82
5	**0.03**	**1**	**ACN**	**Reflux**	**3**	**97**
6	0.04	1	ACN	Reflux	3	97
7	0.03	1	ACN	25	3	56
8	0.03	1	ACN	50	3	71
9	0.03	1	ACN	70	3	82
10	0.03	2	ACN	Reflux	3	60
11	0.03	1	Chloroform	Reflux	3	75
12	0.03	1	Toluene	Reflux	3	60
13	0.03	1	Dioxane	Reflux	3	65
14	0.03	1	n-Hexane	Reflux	3	45

[a] Reaction conditions: 4-methoxybenzyl alcohol (1.0 mmol), TBHP (1.0 mmol) and Fe_3O_4@raffinose-Cu_2O NPs (0.006 g) in 0.5 mL of acetonitrile under refluxing conditions.
[b] Conversion determined by GC using biphenyl as an internal standard.

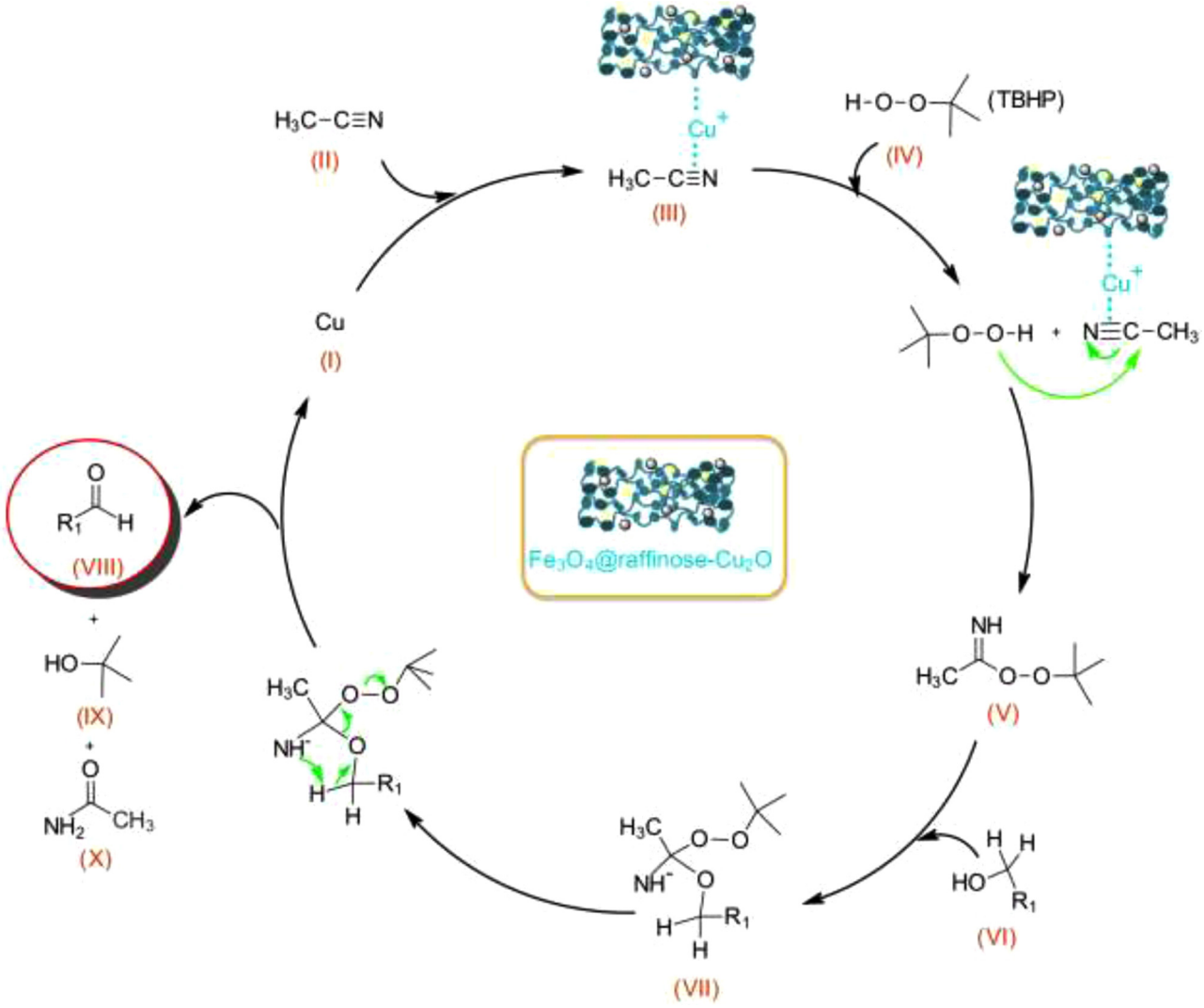

Fig. 9. Proposed mechanism for the selective oxidation of PBA to BAD by using Fe_3O_4@raffinose-Cu_2O NPs.

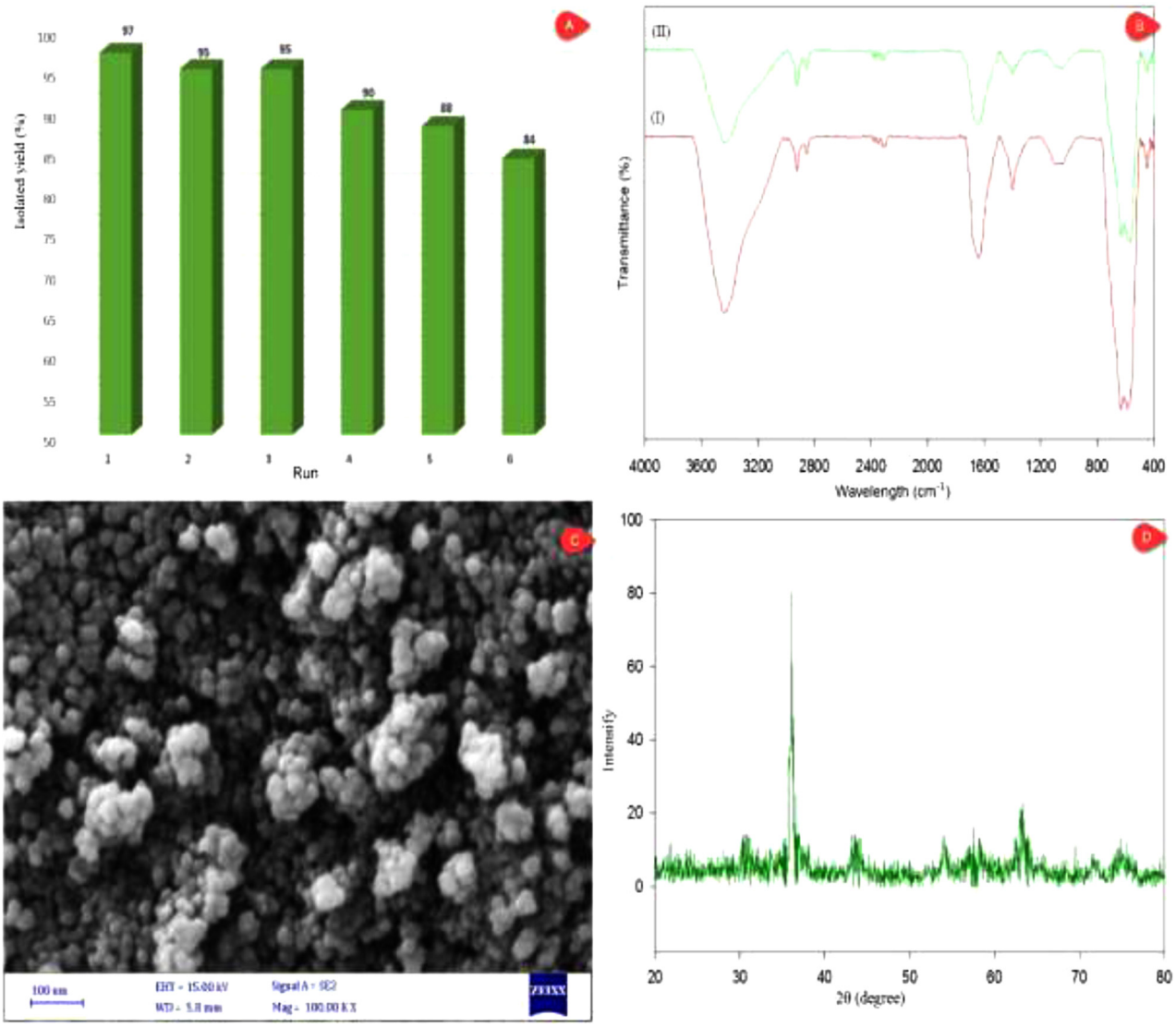

Fig. 10. Reusability (a) diagram (b) FT-IR spectroscopy of (I) magnetic nanocatalyst before used in the reaction, (II) after six times used in the reaction (c) FESEM image (d) XRD pattern of the Fe_3O_4@raffinose-Cu_2O NPs.

Table 3
Comparison of some catalysts effects with Fe_3O_4@raffinose-Cu_2O NPs for the oxidation of 4-methoxybenzyl alcohol to 4-methoxy benzaldehyde.

Entry	Catalyst	Reaction conditions	Time (h)	Yield (%)	Conversion (%)	Selectivity to BAD (%)	Ref.
1	$CoFe_2O_4$@SiO_2@Co(III) salen complex	Acetic acid /60 °C	4	10	–	–	[40]
2	Co(III)@Fe_3O_4@SiO_2 salen complex	Acetonitrile/reflux	3	–	95	99	[41]
3	MCM-41-pr-NH_2-CuL	Acetonitrile/60 °C	3	95	–	–	[42]
4	STA-12(Co)	Ehtylacetate/60 °C	1.5	65	–	> 99	[43]
5	Fe_3O_4@ raffinose-Cu_2O NPs	Acetonitrile/reflux	3	97	97	> 99	This work

administration, Supervision, Validation, Writing - review & editing. **Hossein Ghafuri:** Writing - review & editing.

Declaration of Competing Interest

All authors declare that they have not any conflict of interest in this work.

Acknowledgment

The authors are thankful to the Iran University of Science and Technology.

References

[1] A. Maleki, T. Kari, Novel leaking-free, green, double core/shell, palladium-loaded magnetic heterogeneous nanocatalyst for selective aerobic oxidation, Catal. Lett. 148 (2018) 2929–2934.
[2] A. Maleki, Green oxidation protocol: selective conversions of alcohols and alkenes to aldehydes, ketones and epoxides by using a new multiwall carbon nanotube-based hybrid nanocatalyst via ultrasound irradiation, Ultrason. Sonochem. 40 (2018) 460–464.
[3] A.J. Faqeeh, T.T. Ali, S.N. Basahel, K. Narasimharao, Nanosized samarium modified Au-$Ce_{0.5}Zr_{0.5}O_2$ catalysts for oxidation of benzyl alcohol, Mol. Catal. 456 (2018) 10–21.
[4] A.S. Burange, S.R. Kale, R. Zboril, B. Gawande, R.V. Jayaram, Magnetically retrievable MFe_2O_4 spinel (M = Mn, Co, Cu, Ni, Zn) catalysts for oxidation of benzylic alcohols to carbonyls, RSC Adv. 4 (2014) 6597–6601.

[5] T. Tian, S. Freeman, M. Corey, J.B. German, D. Barile, Chemical characterization of potentially prebiotic oligosaccharides in brewed coffee and spent coffee grounds, J. Agr. Food. Chem. 65 (2017) 2784–2792.

[6] Q. Li, S. Zhou, J. Jing, T. Yang, S. Duan, Z. Wang, Q. Mei, L. Liu, Oligosaccharide from apple induces apoptosis and cell cycle arrest in HT29 human colon cancer cells, Int. J. Biol. Macromol. 57 (2013) 245–254.

[7] N. Liu, Z. Chi, Q. Wang, J. Hong, G. Liu, Z. Hu, Z. Chi, Simultaneous production of both high molecular weight pullulan and oligosaccharides by aureobasdium melanogenum P16 isolated from a mangrove ecosystem, Int. J. Biol. Macromol. 102 (2017) 1016–1024.

[8] A. Pourjavadi, A. Motamedi, S.H. Hosseini, M. Nazari, Magnetic starch nanocomposite as a green heterogeneous support for immobilization of large amounts of copper ions: heterogeneous catalyst for click synthesis of 1,2,3-triazoles, RSC Adv. 6 (2016) 19128–19135.

[9] C. Besset, S. Chambert, Y. Queneau, S. Kerverdo, H. Rolland, J. Guilbot, Reactivity of melezitose and raffinose under Mitsunobu reaction conditions, Carbohydr. Res. 343 (2018) 929–935.

[10] W. Cheng, S. Lin, Processes of dehydration and rehydration of raffinose pentahydrate investigated by thermal analysis and FT-IR/DSC microscopic system, Carbohydr. Polym. 64 (2006) 212–217.

[11] S. Dabral, S. Nishimura, K. Ebitani, One-Pot Conversions of Raffinose into furfural derivatives and sugar alcohols by using heterogeneous catalysts, ChemSusChem. 7 (2014) 260–267.

[12] N.E. Eleraky, A. Allam, S.B. Hassan, M.M. Omar, Nanomedicine fight against antibacterial resistance: an overview of the recent pharmaceutical innovations, Pharmaceutics 12 (2020) 142.

[13] S. Parvaz, R. Taheri-Ledari, M.S. Esmaeili, M. Rabbani, A. Maleki, A brief survey on the advanced brain drug administration by nanoscale carriers: with a particular focus on AChE reactivators, Life Sci. 240 (2020) 117099.

[14] B. Kuswandi, Nanobiosensor approaches for pollutant monitoring, Environ. Chem. Lett. 17 (2019) 975–990.

[15] R.G. Hosh, P.K. Giri, Silicon nanowire heterostructures for advanced energy and environmental applications: a review, Nanotechnology 28 (2017) 012001.

[16] A. Maleki, F. Hassanzadeh-Afruzi, Z. Varzi, M.S. Esmaeili, Magnetic dextrin nanobiomaterial: an organic-inorganic hybrid catalyst for the synthesis of biologically active polyhydroquinoline derivatives by asymmetric Hantzsch reaction, Mater. Sci. Eng. C. 109 (2020) 110502.

[17] A. Maleki, Z. Varzi, F. Hassanzadeh-Afruzi, Preparation and characterization of an eco-friendly $ZnFe_2O_4$@alginic acid nanocomposite catalyst and its application in the synthesis of 2-amino-3- cyano-4H-pyran derivatives, Polyhedron 171 (2019) 193–202.

[18] C. Liang, X. Li, D. Su, Q. Ma, J. Mao, Z. Chen, Y. Wang, J. Yao, H. Li, Magnetic nanostructured cobalt–cobalt oxide/nitrogen-doped carbon material as an efficient catalyst for aerobic oxidation of p-cresols, Mol. Catal. 453 (2018) 121–131.

[19] N. Sgroll, N. Imlyhen, J. Volkman, A.M. Raspolli-Galletti, P. Serp, Copper-based magnetic catalysts for alkyne oxidative homocoupling reactions, Mol. Catal. 438 (2017) 143–151.

[20] M.S. Esmaeili, M.R. Khodabakhshi, A. Maleki, Z. Varzi, Green, natural and low cost Xanthum Gum supported Fe_3O_4 as a robust biopolymer nanocatalyst for the one-pot synthesis of 2-amino-3-cyano-4H-pyran derivatives, Polycycl. Aromat. (2020), https://doi.org/10.1080/10406638.2019.1708418.

[21] Z. Li, S. Wu, C. Yang, Y. Ma, X. Fu, L. Peng, J. Guan, Q. Kan, Nano-Co_3O_4 supported on magnetic N-doped graphene as highly efficient catalyst for epoxidation of alkenes, Mol. Catal. 432 (2017) 267–273.

[22] R.O. Henriques, J.A. Bork, G. Fernandez-Lorente, J.M. Guisan, A. F, D. Oliveira, B.C. Pessel, Co-immobilization of lipases and β-D-galactosidase onto magnetic nanoparticle supports: biochemical characterization, Mol. Catal. 453 (2018) 12–21.

[23] S. R.Chaurasia, A. R.Tiwari, B.M. Bhanage, Synthesis of quinolines via acceptorless dehydrogenative tandem cyclization of 2-amionbenzyl alcohol with alcohols using magnetic CuNiFeO nanocatalyst, Mol. Catal. 478 (2019) 110565.

[24] H. Sharma, S. Sharma, C. Sharma, S. Paul, J.H. Clark, Magnetically recoverable graphene oxide supported Co@Fe_3O_4/L-dopa for C-C cross-coupling and oxidation reactions in aqueous medium, Mol. Catal. 469 (2019) 27–39.

[25] I.D. Hierro, Y. Pérez, M. Fajardo, Silanization of Iron oxide Magnetic Nanoparticles with ionic liquids based on amino acids and its application as heterogeneous catalysts for Knoevenagel condensation reactions, Mol. Catal. 450 (2018) 112–120.

[26] M. Gopiraman, I. Chung, Multifunctional human-hair nanocomposites for oxidation of alcohols, aza -Michael reactions and reduction of 2-nitrophenol, Korean J. Chem. Eng. 34 (2017) 2169–2179.

[27] X. Li, D. Xia, Z. Wen, B. Gong, M. Sun, Y. Wu, J. Zhang, J. Sun, Y. Wu, K. Bao, W. Zhang, Magnetic magnetite nanoparticals catalyzed selective oxidation of α-hydroxy ketones with air and one-pot synthesis of benzilic acid and phenytoin derivatives, Mol. Catal. 454 (2018) 63–69.

[28] P. Basu, P. Bhanja, N. Salam, T.K. Dey, A. Bhaumik, D. Das, S.M. Islam, Silver nanoparticles supported over $Al2O_3$@$Fe2O_3$ core-shell nanoparticles as an efficient catalyst for one-pot synthesis of 1,2,3-triazoles and acylation of benzyl alcohol, Mol. Catal. 439 (2017) 31–40.

[29] F. Li, D. Hu, Y. Yuan, B. Luo, Y. Song, S. Xiao, G. Chen, Y. Fang, F. Lu, Zeolite Y encapsulated Cu (II) and Zn (II)-imidazole-salen catalysts for benzyl alcohol oxidation, Mol. Catal. 452 (2018) 75–82.

[30] A. Maleki, M. Panahzadeh, R. Eivazzadeh-keihan, Agar: a natural and environmentally-friendly support composed of copper oxide nanoparticles for the green synthesis of 1,2,3-triazoles, Green Chem. Lett. Rev. 12 (2019) 395–406.

[31] E. Lagerspets, K. Lagerblom, E. Heliovaara, O.M. Hiltunen, K. Moslova, M. Nieger, T. Repo, Schiff base Cu(I) catalyst for aerobic oxidation of primary alcohols, Mol. Catal. 468 (2019) 75–79.

[32] Q. MeI, H. Liu, Y. Yang, H. Liu, S. Li, P. Zhang, B. Han, Base-free aerobic oxidation of alcohols over copper-based complex under ambient condition, ACS Sustain. Chem. Eng. 6 (2018) 2362–2369.

[33] M. Sarkheil, M. Lashanizadegan, Copper (II) schiff base complex immobilized on superparamagnetic Fe_3O_4@SiO_2 as a magnetically separable nanocatalyst for oxidation of alkenes and alcohols, Appl. Organomet. Chem. 31 (2017) e3726.

[34] S. Shaabani, A.T. Tabatabaei, A. Shaabani, Copper(I) oxide nanoparticles supported on magnetic casein as a bio-supported and magnetically recoverable catalyst for aqueous click chemistry synthesis of 1,4-disubstituted 1,2,3-triazoles, Appl. Organomet. Chem. 31 (2017) e3559.

[35] Z. Varzi, A. Maleki, Design and preparation of ZnS-$ZnFe2O_4$: a green and efficient hybrid nanocatalyst for the multicomponent synthesis of 2,4,5-triaryl-1H-imidazoles, Appl. Organomet. Chem. 33 (2019) e5008.

[36] R. Eivazzadeh-keihan, F. Radinekiyan, A. Maleki, M.S. Bani, M. Azizi, A new generation of star polymer: magnetic aromatic polyamides with unique microscopic flower morphology and in vitro hyperthermia of cancer therapy, J. Mater. Sci. 55 (2020) 319–336.

[37] B. Maleki, H. Natheghi, R. Tayebee, H. Alinezhad, A. Amiri, S.A. Hossieni, S.A.A. Nouri, Synthesis and characterization of nanorod magnetic Co-Fe mixed oxides and its catalytic behavior towards one-pot synthesis of polysubstituted pyridine derivatives, Polycycl. Aromat. (2018), https://doi.org/10.1080/10406638.2018.1469519.

[38] M. Wang, Y. Ni, A. Liu, Fe_3O_4@Resorcinol – Formaldehyde Resin/Cu_2O composite microstructures: solution-phase construction, magnetic performance, and applications in antibacterial and catalytic fields, ACS Omega 2 (2017) 1505–1512.

[39] L. Shu, Y. Shi, An efficient ketone-catalyzed epoxidation using hydrogen peroxide as oxidant, J. Org. Chem. 65 (2010) 8807–8810.

[40] M.A. Nasseri, K. Hemmat, A. Allahresani, E. Hamidi-Hajiabadi, $CoFe_2O_4$@SiO_2@Co (III) salen complex nanoparticle as a green and efficient magnetic nanocatalyst for the oxidation of benzyl alcohols by molecular O_2, Appl. Organomet. Chem. 33 (2019) e4809.

[41] A. Allahresani, M.A. Nasseri, A. Nakhaei, S. Aghajani, Co(III)@Fe_3O_4@SiO_2 salen complex as a highly selective and recoverable magnetic nanocatalyst for the oxidation of sulfides and benzylic alcohols, Iran, Chem. Commun. 7 (2019) 153–169.

[42] M.H. Ardakani, S. Saeednia, P. Iranmanesh, B. Konani, Anchoring of copper(II) Schiff base complex into Aminopropyl-Functionalised MCM-41: a novel, efficient and reusable catalyst for selective oxidation of alcohols, J. Inorg. Organomet. Polym. Mater. 27 (2017) 146–155.

[43] A. Farrokhi, M. Jafarpour, R. Najafzade, Phosphonate-based metal organic frameworks as robust heterogeneous catalysts for TBHP oxidation of benzylic alcohols, Catal. Lett. 147 (2017) 1714–1721.